

Multi-scale interaction among neoclassical tearing mode and drift wave turbulence

M. Yagi 1), S.-I. Itoh 1), K. Itoh 2)

1) Research Institute for Applied Mechanics, Kyushu University, Kasuga, 816-8580, Japan

2) National Institute for Fusion Science, 322-6 Oroshi-cho, Toki, 509-5292, Japan

e-mail contact of main author: yagi@riam.kyushu-u.ac.jp

Abstract. The multi-scale interaction among the tearing mode and the drift wave is investigated using reduced MHD model including the electron viscosity. It is newly found that the fluctuating bootstrap current in the Ohm's law gives rise to a new instability for the regime where the tearing mode is stable. The stability depends on the dissipations and kinetic effects. This result implies that for some parameter regime where Δ' is negative, the seed island may not be needed to drive the neoclassical tearing mode. The nonlinear simulations with multi-helicity modes are performed for the q profile where the (2,1) tearing modes is unstable and for the optimized q profile where all tearing modes are stable. These results are compared with each other.

1. Introduction

The research on the magnetic island in high beta regime is one of important topics in tokamak plasmas. Once it appears, the confinement degradation occurs[1]. Therefore, it is critical to attain the self-ignition condition in International Thermonuclear Experimental Reactor (ITER). The Neoclassical Tearing Mode (NTM) is a possible candidate to drive magnetic island[2,3] in high beta plasmas. The Rutherford type equation is derived to analyze NTM.

The simple form is given by $\frac{G_1}{\eta} \frac{dw}{dt} = \frac{\Delta'}{4} + G_2 \frac{L_q}{L_p} \beta_p \sqrt{\varepsilon} \frac{1}{w}$ where $L_q = q/q'$, $L_p = -p/p'$,

β_p is the poloidal beta and G_1 , G_2 are numerical constants[4,5]. If $\Delta' < 0$, then the

saturated island width is determined by $\frac{dw}{dt} = 0$. For the subcritical bifurcation of magnetic

island, the extra term such as the transport threshold is introduced[6]. The linear stability of

tearing mode with neoclassical effect is analytically investigated in the sheared slab

geometry[7]. It is found that tearing mode tends to be strongly suppressed by the combined

effects of rotation damping in the vorticity equation and the bootstrap current in Ohm's law.

So far, no one investigate numerically the linear stability of tearing mode with neoclassical

effect in the limit of $\Delta' < 0$. This is because in this limit, the tearing mode is considered to be

stable, so is NTM.

In this paper, we examine the linear stability of drift tearing mode with neoclassical effect in

the cylindrical geometry. It is found that there is an instability even in the limit of $\Delta' < 0$ if

the fluctuating bootstrap current is included. This instability is stabilized by the drift effect

and by collisional viscosities. The result implies that for some parameter regime where Δ' is

negative, the seed island may not be needed to drive the neoclassical tearing mode. The

nonlinear simulations with multi-helicity modes are also performed for the q profile where the

(2,1) tearing modes is unstable and for the optimized q profile where all tearing modes are

stable. These results are compared with each other.

2. 3-field Reduced MHD Model

The 3-field reduced MHD model including the neoclassical electron viscosity is derived by neglecting parallel ion momentum equation from the 4-field model[8]. It consists of the vorticity equation, Ohm's law and the continuity equation:

$$\begin{aligned}\frac{d}{dt}U &= \nabla_{\parallel}J + \mu\nabla_{\perp}^2U, \\ \frac{\partial}{\partial t}A &= -\nabla_{\parallel}\phi + \delta\nabla_{\parallel}n - \eta_{\parallel}(1 + \sqrt{\varepsilon})J - \eta_{\parallel}\sqrt{\varepsilon}\frac{q}{\varepsilon}\frac{\partial n}{\partial r}, \\ \frac{dn}{dt} &= \beta\delta\nabla_{\parallel}J + \eta_{\perp}\beta\nabla_{\perp}^2n,\end{aligned}$$

where $d/dt = \partial/\partial t + [\phi, \cdot]$, $[\cdot, \cdot]$ is the Poisson bracket, $\nabla_{\parallel} = ik_{\parallel} - [A, \cdot]$, $U = \nabla_{\perp}^2\phi$, $J = -\nabla_{\perp}^2A$. β is the plasma beta, ε is the inverse aspect ratio, $\delta \equiv (c/\omega_{pi})/a$ is the normalized ion skin depth, where c is the speed of light, ω_{pi} is the ion plasma frequency and a is the minor radius. μ is the ion viscosity, η_{\parallel} and η_{\perp} are the parallel and perpendicular resistivity. The parameter δ indicates the strength of the drift wave coupling. The normalization is the same as those given in Ref.[8,9]. In this model, the neoclassical electron flow is simplified by assuming the neoclassical ion flow is zero. The rotation damping is neglected in the vorticity equation for simplicity. It gives the minimal model to describe NTM dynamics.

3. Linear Analysis

In this section, the linear stability of the collisional drift tearing mode with the neoclassical electron viscosity is investigated. The model q profile is introduced as

$$q(r) = \frac{q_s - q_0}{2^b - 1} \left[(1 + (r/r_s)^a)^b - 1 \right] + q_0,$$

where $a = 3$, $b = 1$, $q_s = 2$. Changing the value of q_0 , the absolute value of Δ' is controlled. Figure 1 shows q profiles in cases with $q_0 = 0.6, 1.0, 1.4$.

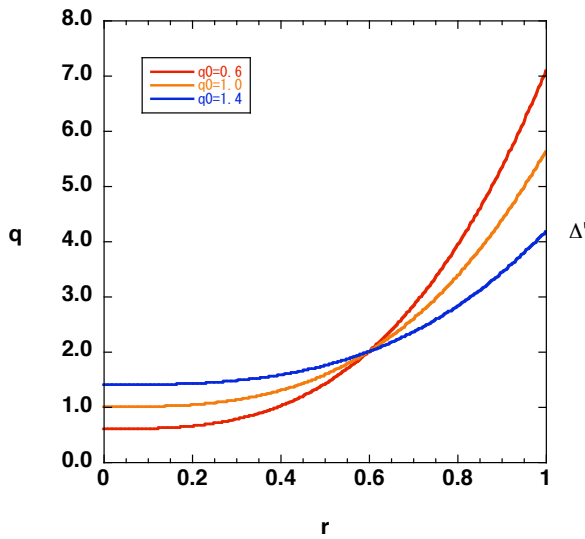


FIG.1. q profiles in cases with $q_0=0.6, 1.0, 1.4$.

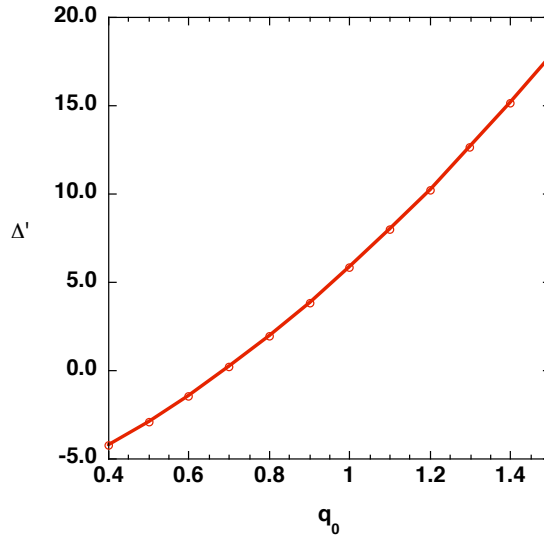


FIG.2. Dependence of Δ' on q_0 .

The corresponding Δ' is shown in figure 2. Simulation parameters are given by $\beta = 10^{-2}$, $\varepsilon = 2 \times 10^{-1}$, $\mu = 10^{-4}$, $\eta_{||} = 10^{-5}$, $\eta_{\perp} = 10^{-4}$. Figure 3 shows the time evolution of electromagnetic energy of (2,1) mode in cases with or without the neoclassical electron viscosity for $\delta = 1.2 \times 10^{-2}$ and $\Delta' = -1.429$. It is shown that even $\Delta' < 0$, the collisional drift tearing mode is unstable for the case with neoclassical electron viscosity.

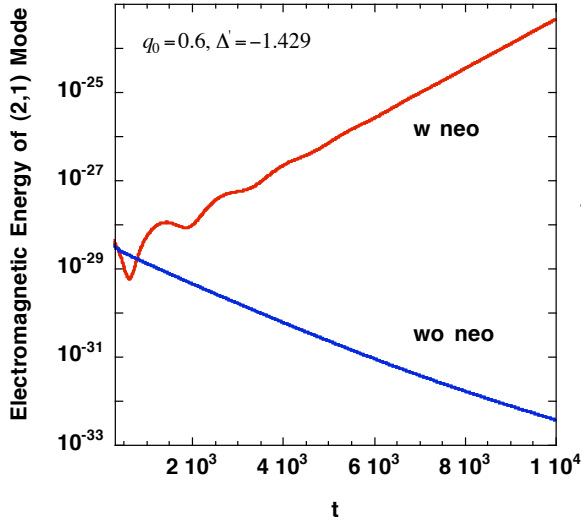


FIG.3. Time evolution of electromagnetic energy of (2,1) mode.

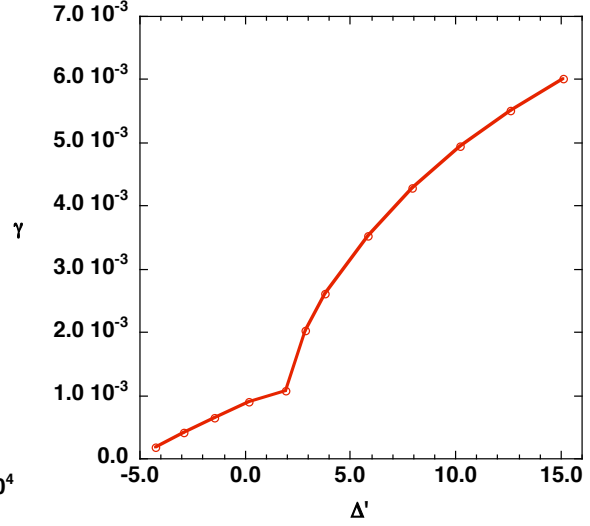


FIG.4. Dependence of growth rate on Δ'

Figure 4 shows the dependence of the growth rate on Δ' in the case with $\delta = 1.2 \times 10^{-2}$. It is found that the collisional drift tearing mode is unstable for the large negative value of Δ' in this case. Next, the dependence of the growth rate on δ is investigated. The result is shown in figure 5. The fitting curve proportional to $e^{-29.126\delta}$ is shown by the dashed curve.

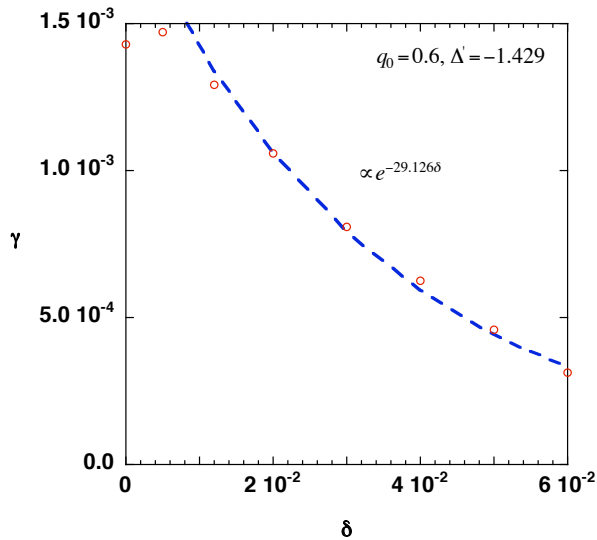


FIG.5. Dependence of growth rate on δ .

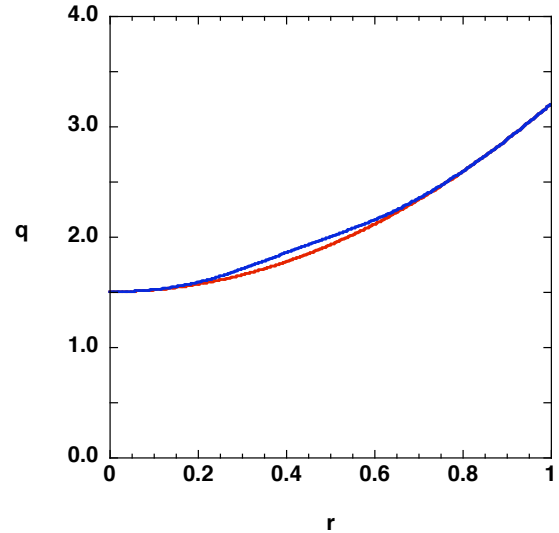


FIG.6. q profiles for nonlinear simulations

It is expected that the complete stabilization can not be attained by only the electron diamagnetic effect in this model. On the other hand, we have already found that the sound

wave stabilizes the collisional drift tearing mode with neoclassical ion and electron viscosity[9] in the banana regime, so that we may speculate that the existence of the stability threshold in $\Delta' < 0$ regime strongly depends on dissipations and kinetic effects. The more precise treatment of these effects is necessary to argue the stability boundary of the instability. It is left for future work.

4. Nonlinear Simulation with Multi-helicity

4.1. q-profile Dependence

In this section, the nonlinear simulations with multi-helicity modes are performed for two different q profiles. Figure 6 shows q profiles used in the nonlinear simulations. The red curve indicates the standard q profile which is unstable for the (2,1) tearing mode, i.e., $\Delta'_{2/1} = 11.1$ and the blue curve indicates the optimized q profile which is stable for all tearing modes, $\Delta'_{2/1} = -0.244$. Simulation parameters are the same as those used in the linear analysis except $\delta = 1.2 \times 10^{-2}$. Figure 7 and 8 show time evolution of electromagnetic energy of each Fourier mode in cases with the standard q profile and the optimized q profile.

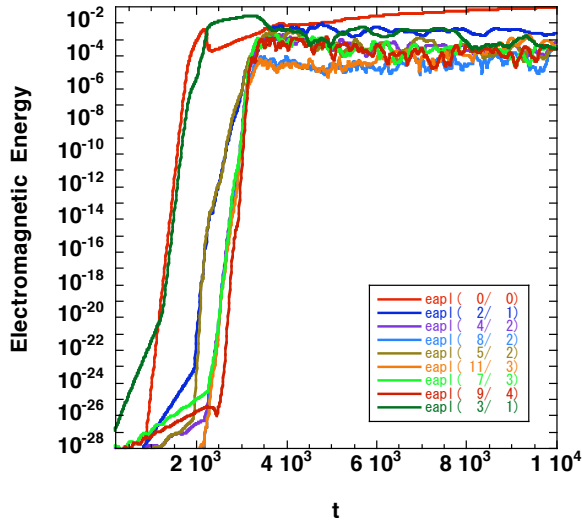


FIG.7. Time evolution of electromagnetic energy for standard q profile.

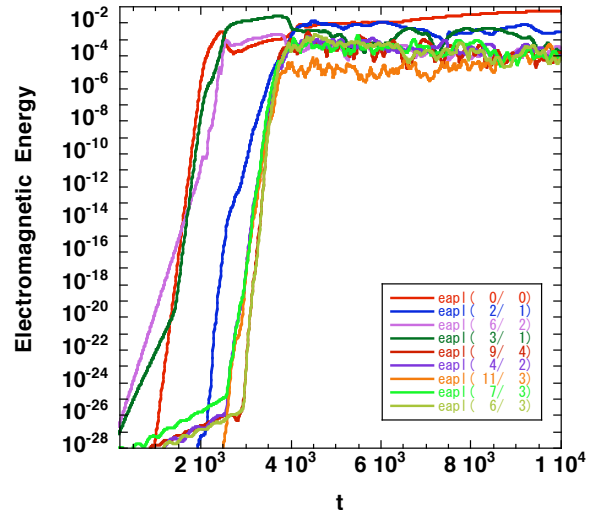


FIG.8. Time evolution of electromagnetic energy for optimized q profile.

For the standard q profile, the (3,1) collisional drift tearing mode with neoclassical electron viscosity linearly grows at $t \leq 1000$, then it is nonlinearly accelerated due to the three wave coupling of high m modes at $1000 \leq t \leq 2000$. The nonlinear acceleration mechanism is explained based on the kick of turbulent noise[10]. It enters the Rutherford regime and then saturates at $t \approx 2200$. The (2,1) mode appears later time since the linear growth rate is smaller than that of (3,1) mode, then it is nonlinearly accelerated at $t \approx 2000$. It saturates at $t \approx 3500$. In the later saturation phase, at $4000 \leq t \leq 8000$, the (2,1) mode interacts with (3,1) mode. The (0,0) mode dominates the system in the saturation phase. For the optimized q profile, the (6,3) mode is linearly unstable in the initial phase, however, in the saturation phase, the tendency of mode behavior is similar to the standard q profile, so that we discuss the results in the optimized q profile in the following subsection.

4.2. Nonlinear Dynamics

In this subsection, we examine the behavior of each mode in the saturation phase. Figure 9 and 10 show the contour plot of $A(r, \theta, z = 0)$ at $t = 8000$ and $t = 10000$, respectively. At $t = 8000$, the (2,1) mode strongly interact with (3,1) mode and at $t = 10000$, the (2,1) mode is dominant as is seen in Fig.8. This is also observed in the contour plot of $A(r, \theta, z = 0)$, where the structure changes in each time.

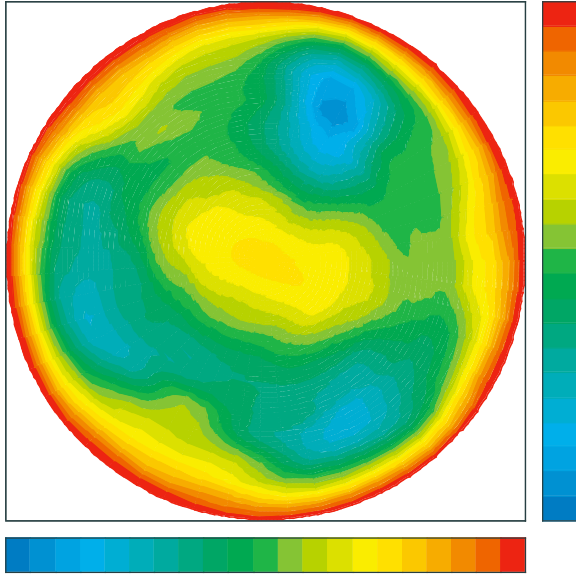


FIG. 9. Contour plot of $A(r, \theta, z = 0)$ at $t = 8000$.

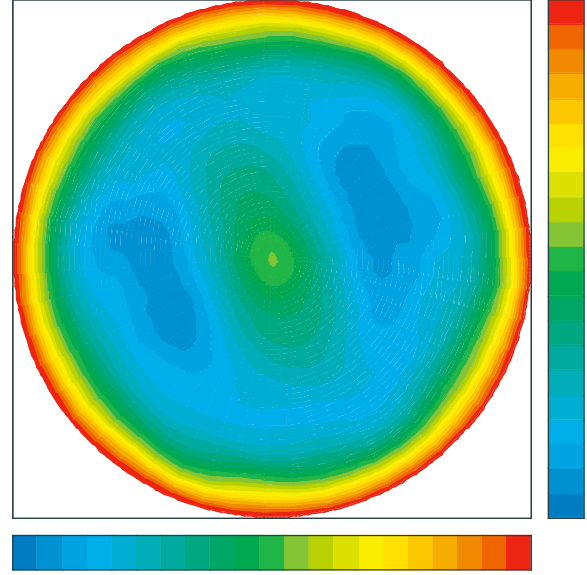


FIG.10. Contour plot of $A(r, \theta, z = 0)$ at $t = 10000$.

Next, we evaluate the particle flux $\Gamma(r) = \langle nv_{E \times B} \rangle$, where the bracket indicates the average in the poloidal and toroidal direction. Figure 11 shows the radial profile of the particle flux in the saturation phase. At $t = 8000$, the negative peak appears around $r = 0.5$, on the other hand, at $t = 10000$, the positive peak appears in the same region. The nonlinear interaction between (2,1) and (3,1) modes generate the negative flux in this region.

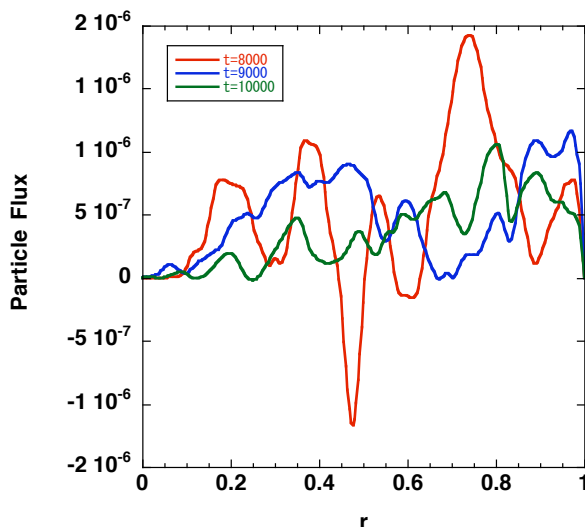


FIG.11 Radial profile of particle flux.

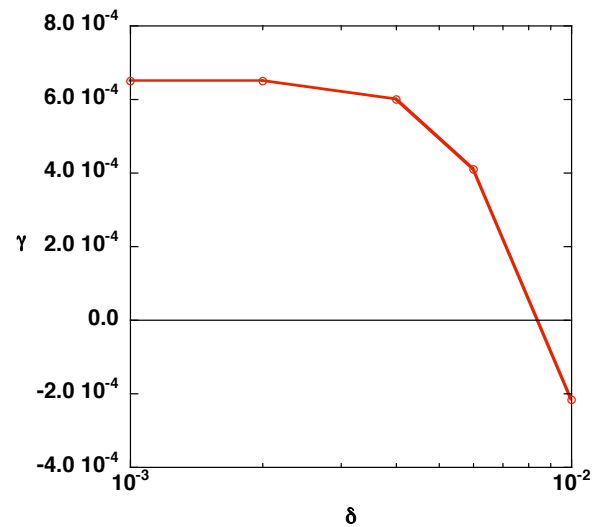


FIG.12 Dependence of growth rate on δ .

Unfortunately, only 343 Fourier modes are taken into account in this simulation so that it is difficult to argue the transport driven by the interaction between tearing mode and high m turbulence. It is left as a future work.

5. 4-field Reduced MHD Model

In the section 3, we do not find the stability threshold of the collisional drift tearing mode described by the three-field model, so that we extend the model in this section. The 4-field model is derived by assuming cold ion and neglecting parallel ion momentum:

$$\begin{aligned} \frac{d}{dt} \nabla_{\perp}^2 \phi &= -\nabla_{\parallel} \nabla_{\perp}^2 A + \mu_{\perp} \nabla_{\perp}^4 \phi, \\ \frac{\partial}{\partial t} A &= -\nabla_{\parallel} (\phi - \delta p) + \alpha_T \delta \nabla_{\parallel} T + \eta_{\parallel} (1 + \sqrt{\varepsilon}) \nabla_{\perp}^2 A - \eta_{\parallel} \sqrt{\varepsilon} \frac{q}{\varepsilon} \frac{\partial p}{\partial r}, \\ \frac{d}{dt} n + \beta \frac{d}{dt} p &= -\beta \delta \nabla_{\parallel} \nabla_{\perp}^2 A + \eta_{\perp} \beta \nabla_{\perp}^2 p - \beta \eta_{\parallel} \sqrt{\varepsilon} \frac{1}{r} \frac{\partial}{\partial r} r \nabla_{\perp}^2 A + \beta \eta_{\parallel} \sqrt{\varepsilon} \frac{q}{\varepsilon} \frac{1}{r} \frac{\partial}{\partial r} r \frac{\partial p}{\partial r}, \\ \frac{3}{2} \frac{d}{dt} T - \frac{d}{dt} n &= -\alpha_T \delta \beta \nabla_{\parallel} \nabla_{\perp}^2 A + \chi_{\perp} \nabla_{\perp}^2 T. \end{aligned}$$

In this extension, we include the neoclassical electron viscosities in the continuity equation which are neglected in the 3-field model. In addition, we include the electron temperature evolution equation where $\alpha_T = 0.71$ and $\chi_{\perp} = 10^{-4}$. Using the optimized q profile introduced in the section 4, we investigate the stability threshold of the collisional drift tearing mode. Figure 12 shows the dependence of growth rate on δ . It is found that the stability threshold strongly depends on η_{\perp} and χ_{\perp} . If we set $\eta_{\perp} = \chi_{\perp} = 0$, no stability threshold is found and higher harmonics are more unstable than (2,1) mode. In addition, the neoclassical electron viscosities in the continuity equation are also important. Without them, the stability threshold disappears even if η_{\perp} and χ_{\perp} are finite.

6. Nonlinear Simulation with Single-helicity

In this section, the nonlinear simulation with single-helicity is performed using 4-field model. Adapting eigen-functions obtained by the simulation with standard q profile as initial values, we restart the run with the optimized q profile and observe the dynamics of NTM. Figures 13 shows the time evolution of electromagnetic energy of (2,1) mode in case with $\delta = 10^{-2}$, where mode is linearly stable as is shown in Fig.12. It is found that the nonlinear sustainment does not occur but the magnetic island simply dumps out in this case. This result is different from that given by a simple Rutherford model, where the magnetic island will grow if $\Delta' < 0$ and the seed island is given initially. In our model, the dissipations play important role to determine the stability threshold of the collisional drift tearing mode in $\Delta' < 0$ regime. Therefore, it is difficult to argue the sub-critical excitation of NTM based on our model at this point. Instead, we should clarify the mechanism of island saturation (the simple balance between Δ' and the fluctuating bootstrap current term does not explain simulation results, since the quasi-linear effect is more prominent). It is left as a future work.

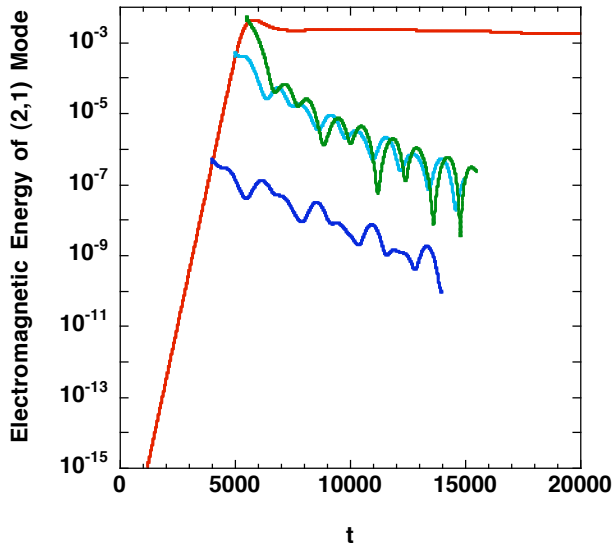


FIG.13. Time evolution of electromagnetic energy.

References

- [1] SAUTER, O., et al., "Beta limits in long-pulse tokamak discharges", *Phys. Plasmas* **4** (1997) 1654.
- [2] CARRERA, R., et al., "Island bootstrap current modification of the nonlinear dynamics of the tearing mode", *Phys. Fluids* **29** (1986) 899.
- [3] CALLEN, J. D., et al., "Neoclassical MHD equations, instabilities and transport in tokamaks", *Plasma Physics and Controlled Nuclear Fusion Research*, Kyoto, IAEA, Vienna (1987), Vol.2 p.157.
- [4] SMOLYAKOV, A., "Nonlinear evolution of tearing modes in inhomogeneous plasmas", *Plasma Phys. Controlled Fusion* **35** (1993) 657.
- [5] FURUYA, A., et al., "Effects of Microscopic Turbulence on Magnetic Island", *J. Phys. Soc. Jpn.* **71** (2002) 1261.
- [6] FITZPATRICK, R., "Helical temperature perturbations associated with tearing modes in tokamak plasmas", *Phys. Plasmas* **2** (1995) 825.
- [7] HAHM, T. S., "Neoclassical tearing modes in a tokamak", *Phys. Fluids* **31** (1988) 3709.
- [8] YAGI, M., et al., "Nonlinear simulation of tearing mode based on 4-field RMHD model", *Nucl. Fusion* **45** (2005) 900.
- [9] FURUYA, A., et al., "Linear analysis of neoclassical tearing mode based on the four-field reduced neoclassical MHD equation", *J. Phys. Soc. Jpn.* **72** (2003) 313.
- [10] YAGI, M. et al., "Nonlinear drive of tearing mode by microscopic plasma turbulence", *Plasma and Fusion Res.* **2** (2007) 025.